

Linear NMR in the polar phase of ^3He in aerogel

V. V. Zavjalov¹⁾,

Low Temperature Laboratory, Department of Applied Physics, Aalto University, PO Box 15100, FI-00076 AALTO, Finland

^3He is an example of the system with non-trivial Cooper pairing. A few different superfluid phases are known in this system. Recently the new one, the polar phase, have been observed in ^3He confined in nematically ordered aerogel. A number of various topological defects including half-quantum vortices can exist the polar phase. In this work we present theoretical and numerical studies of linear NMR in the polar phase both in the uniform order-parameter texture and in the presence of half-quantum vortices.

Introduction

The polar phase of ^3He in nematically ordered aerogel has been predicted in [1] and found experimentally in [2]. In this system a new topological defect, a half-quantum vortex can exist. Half-quantum vortices have been originally predicted for A-phase in [3] but have not been observed in experiments. This is because of energetically unfavorable solitons which should always connect half-quantum vortex pairs in the A-phase. In the polar phase of ^3He in aerogel there are no such solitons if the magnetic field is parallel to aerogel strands. Also vortices in the polar phase are strongly pinned and cannot move when the field is tilted and solitons appear. In our experimental work [4] vortices were created by rotating the ^3He sample. Then the field was tilted and spin waves localized in solitons were observed by NMR. In this paper we develop a theory for textures, topological defects and spin dynamics in the polar phase of ^3He . We also do numerical simulations of spin waves in the presence of half-quantum vortices.

Order-parameter and energies

We are studying the polar phase of ^3He in nematically ordered aerogel. The order parameter in this system ([5]) is

$$A_{aj} = \frac{1}{\sqrt{3}} \Delta e^{i\varphi} d_a l_j, \quad (1)$$

where φ is the phase, and \mathbf{d} and \mathbf{l} are unit vectors in spin and orbital spaces respectively. The orbital unit vector \mathbf{l} is directed along the aerogel strands and can not move.

There are three components of the Hamiltonian which are important for spin dynamics: magnetic energy, energy of spin-orbit interaction and gradient energy:

$$\mathcal{H} = F_M + F_{SO} + F_{\nabla}, \quad (2)$$

$$F_M = -(\mathbf{S} \cdot \gamma \mathbf{H}) + \frac{\gamma^2}{2} \chi_{ab}^{-1} S_a S_b, \quad (3)$$

$$F_{SO} = 3g_D \left[A_{jj}^* A_{kk} + A_{jk}^* A_{kj} - \frac{2}{3} A_{jk}^* A_{jk} \right], \quad (4)$$

$$F_{\nabla} = \frac{3}{2} \left[K_1 (\nabla_j A_{ak}^*) (\nabla_j A_{ak}) + K_2 (\nabla_j A_{ak}^*) (\nabla_k A_{aj}) + K_3 (\nabla_j A_{aj}^*) (\nabla_k A_{ak}) \right], \quad (5)$$

where \mathbf{S} is spin and \mathbf{H} is the magnetic field. Susceptibility χ_{ab} is anisotropic, the axis of anisotropy is \mathbf{d} and minimum of the magnetic energy corresponds to $\mathbf{S} \perp \mathbf{d}$. This can be written as

$$\chi_{ab}^{-1} = \frac{1}{\chi_{\perp}} (\delta_{ab} + \delta d_a d_b), \quad \delta = (\chi_{\perp} - \chi_{\parallel}) / \chi_{\parallel} > 0. \quad (6)$$

Substituting the order parameter (1) into energies and using the fact that \mathbf{l} is uniform we have

$$F_M = -(\mathbf{S} \cdot \gamma \mathbf{H}) + \frac{\gamma^2}{2\chi_{\perp}} [\mathbf{S}^2 + \delta (\mathbf{d} \cdot \mathbf{S})^2], \quad (7)$$

$$F_{SO} = 2\Delta^2 g_D \left[(\mathbf{d} \cdot \mathbf{l})^2 - \frac{1}{3} \right], \quad (8)$$

$$F_{\nabla} = \frac{\Delta^2}{2} K_{jk} [(\nabla_j \varphi)(\nabla_k \varphi) + (\nabla_j d_a)(\nabla_k d_a)], \quad (9)$$

where symmetric matrix $K_{jk} = K_1 \delta_{jk} + (K_2 + K_3) l_j l_k$ is introduced. Motion of the phase φ (sound) is not coupled with the motion of \mathbf{d} (spin waves). In spin dynamics terms with the phase gradients give only a constant contribution to the energy and can be skipped.

Equilibrium texture

Let's first study the static picture. In the equilibrium $\partial \mathcal{H} / \partial S_a = 0$. This means

$$\mathbf{S}^0 + \delta (\mathbf{d}^0 \cdot \mathbf{S}^0) \mathbf{d}^0 = \frac{\chi_{\perp}}{\gamma} \mathbf{H}, \quad (10)$$

where \mathbf{S}^0 and \mathbf{d}^0 are equilibrium values of \mathbf{S} and \mathbf{d} . Multiplying this by \mathbf{d}^0 we can find $(\mathbf{d}^0 \cdot \mathbf{S}^0) = \chi_{\parallel} / \gamma (\mathbf{d}^0 \cdot \mathbf{H})$.

¹⁾e-mail: vladislav.zavjalov@aalto.fi

then substituting it back to (10) we find the value for the spin in the equilibrium:

$$\gamma S_a^0 = [\chi_\perp \delta_{ab} - (\chi_\perp - \chi_\parallel) d_a^0 d_b^0] H_b = \chi_{ab} H_b \quad (11)$$

For calculation of the equilibrium distribution (texture) of the \mathbf{d} vector we will use a coordinate system where $\mathbf{H} \parallel \hat{\mathbf{z}}$ and \mathbf{l} is in $\hat{\mathbf{z}} - \hat{\mathbf{y}}$ plane (See Fig.1). This can be written as

$$\begin{aligned} \mathbf{H} &= \hat{\mathbf{z}} H, & \mathbf{l} &= \hat{\mathbf{y}} \sin \mu + \hat{\mathbf{z}} \cos \mu, \\ \mathbf{d}^0 &= (\hat{\mathbf{x}} \cos \alpha + \hat{\mathbf{y}} \sin \alpha) \sin \beta + \hat{\mathbf{z}} \cos \beta. \end{aligned} \quad (12)$$

Here μ is angle between \mathbf{l} and magnetic field, it is set by the experimental setup because direction of \mathbf{l} is determined by aerogel; β is angle between \mathbf{d}^0 and the field; α is azimuthal angle of \mathbf{d} in the plane, perpendicular to the magnetic field, it is counted from the line, perpendicular to both \mathbf{H} and \mathbf{l} which corresponds to the minimum of energy.

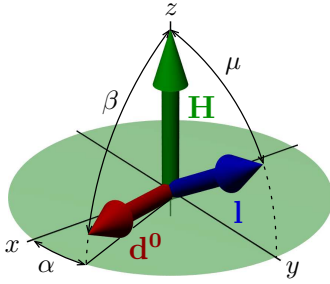


Fig. 1. Angles, used in the texture calculations

The energies (7)-(9) (without constant terms) are:

$$F_M = \frac{1}{2}(\chi_\perp - \chi_\parallel) H^2 \cos^2 \beta, \quad (13)$$

$$F_{SO} = 2g_D \Delta^2 (\sin \alpha \sin \beta \sin \mu + \cos \beta \cos \mu)^2, \quad (14)$$

$$F_\nabla = \frac{\Delta^2}{2} K_{jk} [\sin^2 \beta (\nabla_j \alpha)(\nabla_k \alpha) + (\nabla_j \beta)(\nabla_k \beta)] \quad (15)$$

There are two scales introduced by these energies. Ratio of magnetic and gradient energies gives the magnetic length ξ_H and ratio of spin-orbit and gradient energies gives the dipolar length ξ_D . Since the gradient energy is anisotropic, we have different values in directions perpendicular and parallel to the \mathbf{l} vector:

$$\xi_{Hjk}^2 = \frac{K_{jk} \Delta^2}{H^2 (\chi_\perp - \chi_\parallel)}, \quad \xi_{Djk}^2 = \frac{K_{jk}}{4g_D} \quad (16)$$

In the high-field limit $\xi_D \gg \xi_H$. Magnetic energy is in the minimum everywhere excluding small regions of the ξ_H size (for example cores of spin vortices). The

small volume of this regions makes them invisible in NMR experiments. In the rest of the volume $\beta = \pi/2$, only variations of α are important and the energy is:

$$\mathcal{H} = \frac{1}{2} K_{jk} \Delta^2 (\nabla_j \alpha)(\nabla_k \alpha) + 2g_D \Delta^2 \sin^2 \alpha \sin^2 \mu \quad (17)$$

The equilibrium state corresponds to the minimum: $\delta \mathcal{H} / \delta \alpha = 0$. Since the energy depends on the gradient we have to use variational derivative

$$\frac{\delta \mathcal{H}}{\delta \alpha} = \frac{\partial \mathcal{H}}{\partial \alpha} - \nabla_j \frac{\partial \mathcal{H}}{\partial \nabla_j \alpha}. \quad (18)$$

Using this for energy (17) we have a simple equation for the distribution of α :

$$\bar{\xi}_{jk}^2 \nabla_j \nabla_k \alpha = \frac{1}{2} \sin 2\alpha, \quad (19)$$

$$\text{where } \bar{\xi}_{jk} = \frac{\xi_{Djk}}{\sin \mu}.$$

One can see that in the case of $\mathbf{H} \parallel \mathbf{l}$ (or $\mu = 0$) there is no length scale in this problem. \mathbf{d} can freely move in the plane perpendicular to the field and only the gradient term is important. Tilting the magnetic field from the \mathbf{l} direction makes the length $\bar{\xi}$ finite. At $\mathbf{H} \perp \mathbf{l}$ the length scale reaches its minimum value, ξ_D .

Textural defects

Equation (19) shows that in a tilted magnetic field there are two possible uniform textures with $\alpha = 0$ and $\alpha = \pi$. Vector \mathbf{d} is oriented perpendicularly to both \mathbf{H} and \mathbf{l} and can point in two possible directions. Between this two states there is a *d-soliton*. One can also imagine a *spin vortex* in which vector \mathbf{d} rotates by 2π around the vortex line. Two *d-solitons* should end at this vortex. Looking at the order parameter formula (1) one can see that there can be also a *half-quantum vortex*, in which both vector \mathbf{d} and phase ϕ rotate by π around the vortex line. This is possible because $A_{\alpha j}(\mathbf{d}, \phi) = A_{\alpha j}(-\mathbf{d}, \phi + \pi)$. In the tilted magnetic field one *d-soliton* should end at the half-quantum vortex. On Fig. 2 two types of vortices are shown.

The form of the single *d-soliton* can be found analytically. In this one-dimensional problem equation (19) has a form of static sine-Gordon equation:

$$\bar{\xi}^2 \alpha''(x) = \frac{1}{2} \sin 2\alpha(x), \quad (20)$$

where x is a coordinate perpendicular to the soliton. Here the value of $\bar{\xi}$ depends on the soliton orientation: if x coordinate goes perpendicular or parallel to \mathbf{l} , it should be $\bar{\xi}_\perp$ or $\bar{\xi}_\parallel$ respectively.

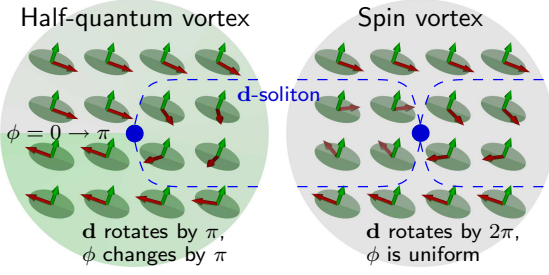


Fig. 2. The half-quantum vortex and the spin vortex in the polar phase of ^3He . Vector \mathbf{l} is perpendicular to the picture plane. Angle $\alpha = 0$ is changing by π between upper and lower parts of the picture. This can be done via either a d -soliton or a π jump in the phase (which is shown by color gradient).

The analytical solution can be obtained by multiplying the equation by a' and integrating with proper boundary conditions. Then for a single soliton with $\sin \alpha(\pm\infty) = 0$ and $\alpha'(\pm\infty) = 0$ we have

$$\bar{\xi}^2 (\alpha')^2 = \sin^2 \alpha, \quad (21)$$

and then for the soliton located at $x = 0$:

$$\alpha(x) = 2 \arctan(\exp(x/\bar{\xi})) \quad (22)$$

In the 2D case with isotropic ξ_D (which takes place when the texture is uniform along \mathbf{l} -direction) the sine-Gordon equation has analytic solutions for a number of configurations with spin vortices and solitons [6, 7]. This includes, in particular, the kink on soliton, which represents the one-quantum (2π) spin vortex with two d -solitons being on the opposite sides of it (see right part of Fig. 2). The linear chain of the alternating 2π and -2π vortices has also analytic solution. The configuration with two solitons crossing each other may also represent the spin vortex, if each soliton has a kink and the positions of two kinks coincide. This is 4π spin vortex, from which four d -solitons emerge. Such analytic solutions do not take into account the pinning of vortices which exists in the real system.

Spin dynamics

To study spin dynamics we write Hamilton equations using Poisson brackets. Motion of any value A in this approach is given by $\dot{A} = \{\mathcal{H}, A\}$. Choice of coordinates is quite arbitrary as far as we know Poisson brackets for them. Brackets can be found from microscopic considerations, from commutation rules in quantum mechanics, or from symmetry [8]. For spin \mathbf{S} and a vector \mathbf{d} in the spin space the Poisson brackets are

$$\{S_a, S_b\} = -e_{abc} S_c, \quad \{d_a, d_b\} = 0, \quad (23)$$

$$\{d_a, S_b\} = \{S_a, d_b\} = -e_{abc} d_c,$$

and equations of motion:

$$\dot{S}_a = \{\mathcal{H}, S_a\} = \frac{\delta \mathcal{H}}{\delta S_b} \{S_b, S_a\} + \frac{\delta \mathcal{H}}{\delta d_b} \{d_b, S_a\} \quad (24)$$

$$= \frac{\delta \mathcal{H}}{\delta \mathbf{S}} \times \mathbf{S} + \frac{\delta \mathcal{H}}{\delta \mathbf{d}} \times \mathbf{d},$$

$$\dot{d}_a = \{\mathcal{H}, d_a\} = \frac{\delta \mathcal{H}}{\delta S_b} \{S_b, d_a\} + \frac{\delta \mathcal{H}}{\delta d_b} \{d_b, d_a\} \quad (25)$$

$$= \frac{\delta \mathcal{H}}{\delta \mathbf{S}} \times \mathbf{d}.$$

Using these equations one can show that $\frac{d}{dt}(\mathbf{d} \cdot \mathbf{S}) = 0$ and thus the value $(\mathbf{d} \cdot \mathbf{S})$ is an integral of motion.

Derivatives of the Hamiltonian are:

$$\frac{\delta \mathcal{H}}{\delta S_a} = -\gamma H_a + \frac{\gamma^2}{\chi_\perp} [S_a + \delta (\mathbf{d} \cdot \mathbf{S}) d_a], \quad (26)$$

$$\frac{\delta \mathcal{H}}{\delta d_a} = \frac{\delta \gamma^2}{\chi_\perp} (\mathbf{d} \cdot \mathbf{S}) S_a + 4g_D \Delta^2 (\mathbf{d} \cdot \mathbf{l}) l_a - K_{jk} \Delta^2 (\nabla_j \nabla_k d_a). \quad (27)$$

Substituting (26), (27), and (23) into equations (24-25) one has:

$$\dot{\mathbf{S}} = [\mathbf{S} \times \gamma \mathbf{H}] \quad (28)$$

$$+ 4g_D \Delta^2 (\mathbf{d} \cdot \mathbf{l}) [\mathbf{l} \times \mathbf{d}] - K_{jk} \Delta^2 [\nabla_j \nabla_k \mathbf{d} \times \mathbf{d}],$$

$$\dot{\mathbf{d}} = \gamma \left[\mathbf{d} \times \left(\mathbf{H} - \frac{\gamma}{\chi_\perp} \mathbf{S} \right) \right]. \quad (29)$$

Note that the anisotropy of susceptibility does not affect spin dynamics.

Linearized dynamics

Consider small oscillations near the equilibrium:

$$\mathbf{S} = \mathbf{S}^0 + \delta \mathbf{S}(t), \quad \mathbf{d} = \mathbf{d}^0 + \delta \mathbf{d}(t) \quad (30)$$

Linearize equations, differentiate the first one and exclude $\delta \mathbf{d}$. The result can be written as:

$$\delta \ddot{\mathbf{S}}_a = [\delta \dot{\mathbf{S}} \times \gamma \mathbf{H}]_a + \Lambda_{ab} \delta S_b, \quad (31)$$

where we introduce

$$\Lambda_{ab} = \Omega_P^2 [(\mathbf{d}^0 \cdot \mathbf{l})^2 \delta_{ab} - [\mathbf{l} \times \mathbf{d}^0]_a [\mathbf{l} \times \mathbf{d}^0]_b - (\mathbf{d}^0 \cdot \mathbf{l}) d_a^0 l_b] + c_{jk}^2 [(\delta_{ab} - d_a^0 d_b^0) \nabla_j \nabla_k - 2d_b^0 (\nabla_j d_a^0) \nabla_k + d_a^0 (\nabla_j \nabla_k d_b^0) - d_b^0 (\nabla_j \nabla_k d_a^0)], \quad (32)$$

$$\Omega_P^2 = 4g_D \frac{\Delta^2 \gamma^2}{\chi_\perp}, \quad c_{jk}^2 = K_{jk} \frac{\Delta^2 \gamma^2}{\chi_\perp} = \Omega_P^2 \xi_{Djk}^2, \quad (33)$$

and use the fact that $c_{jk} = c_{kj}$. Here Ω_P is analog of Leggett frequency, it determines NMR frequency shifts

caused by spin-orbit interaction and c_{jk} is anisotropic spin-wave velocity.

Consider $H \parallel \hat{z}$ and look for a harmonic solution $\delta \mathbf{S} = \mathbf{s} \exp(i\omega t)$. Then the equation can be written as

$$\begin{aligned} -\omega^2 s_x &= \Lambda_{xb} s_b + i\omega_L \omega s_y, \\ -\omega^2 s_y &= \Lambda_{yb} s_b - i\omega_L \omega s_x, \\ -\omega^2 s_z &= \Lambda_{zb} s_b \end{aligned} \quad (34)$$

In high field (comparing with dipolar and gradient effects) motion of the spin is close to a Larmor precession with frequency $\omega \approx \omega_L = \gamma H$ and $\Lambda \ll \omega_L^2$. One can separate equations by putting s_y from the second equation to the first one and vice versa and neglecting small terms. We get the same equations for s_x and s_y . This can be written as a single equation for a complex coordinate $s_+ = (s_x + is_y)/\sqrt{2}$:

$$(\omega_L^2 - \omega^2)s_+ = i(\Lambda_{xy} - \Lambda_{yx})s_+ + (\Lambda_{xx} + \Lambda_{yy})s_+ \quad (35)$$

In high field \mathbf{d}^0 is perpendicular to the field and we can use angles (12) with $\beta_n = \pi/2$. Then

$$\begin{aligned} \Lambda_{xx} + \Lambda_{yy} &= \Omega_P^2 [(1 + \sin^2 \alpha) \sin^2 \mu - 1] + c_{jk}^2 \nabla_j \nabla_k \\ \Lambda_{xy} - \Lambda_{yx} &= -\frac{1}{2} \Omega_P^2 \sin 2\alpha \sin^2 \mu \\ &\quad + 2c_{jk}^2 [(\nabla_j \nabla_k \alpha) + (\nabla_j \alpha) \nabla_k]. \end{aligned} \quad (36)$$

Substituting this into (35) and using (19) we have

$$\begin{aligned} (\omega^2 - \omega_L^2)s_+ &= \Omega_P^2 \left\{ \cos^2 \mu - \sin^2 \alpha \sin^2 \mu \right\} s_+ \\ &\quad - c_{jk}^2 \left\{ \nabla_j \nabla_k + i[(\nabla_j \nabla_k \alpha) + 2(\nabla_j \alpha) \nabla_k] \right\} s_+. \end{aligned} \quad (37)$$

One can rewrite the equation in the form:

$$\begin{aligned} (\omega^2 - \omega_L^2)s_+ &= \Omega_P^2 \left\{ \cos^2 \mu - \sin^2 \alpha \sin^2 \mu \right\} s_+ \\ &\quad - c_{jk}^2 \left\{ -\left(\frac{\nabla}{i} + \nabla \alpha\right)_{jk}^2 + (\nabla \alpha)_{jk}^2 \right\} s_+. \end{aligned} \quad (38)$$

where we use notation $(X)_{jk}^2 = X_j X_k$. This is similar to the equation of motion of a charged particle in a magnetic field with a vector potential $\mathbf{A} = \nabla \alpha$. The magnetic field $\nabla \times \mathbf{A}$ is zero everywhere except half-quantum vortex cores but it affects the motion of the spin wave because of Aharonov-Bohm effect [9]. This effect for half-quantum vortices in $^3\text{He-A}$ is discussed in [10]. NMR and spin dynamics of half-quantum vortices He-A are calculated in [11].

For numerical calculations it is useful to make a substitution $\bar{s}_+ = s_+ \exp(i\alpha)$. Then the equation for \bar{s}_+ contains no imaginary terms:

$$\begin{aligned} (\omega^2 - \omega_L^2)\bar{s}_+ &= \Omega_P^2 \left\{ \cos^2 \mu - \sin^2 \alpha \sin^2 \mu \right\} \bar{s}_+ \\ &\quad - c_{jk}^2 \left\{ \nabla_j \nabla_k + (\nabla_j \alpha)(\nabla_k \alpha) \right\} \bar{s}_+, \end{aligned} \quad (39)$$

The inverse transformation is needed if one need to calculate the actual distribution of magnetization.

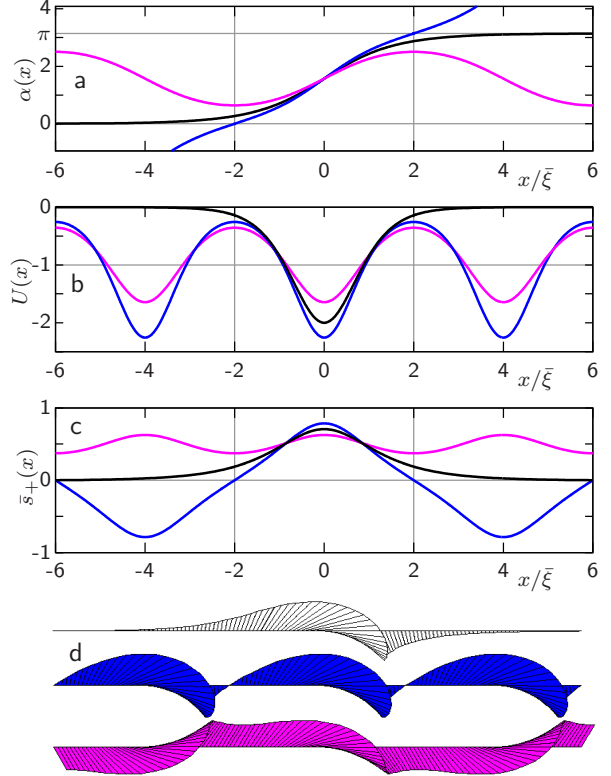


Fig. 3. An example of the calculated texture and the spin wave in 1D soliton structures. Black curves correspond to a single soliton, blue and purple ones correspond to periodic structures with same and alternating soliton orientations and periods $D = 4\xi$. (a) Texture, $\alpha(x)$. (b) Potential for a real-value wave \bar{s}_+ . Energy levels for all three textures are the same, $\lambda = -1$. (c) The real-value wave \bar{s}_+ . (d) Distribution of the amplitude and phase of the actual magnetization $s_+ = \bar{s}_+ \exp(-i\alpha)$. In all three cases the total magnetization $|\int s_+ dx|$ is non-zero.

NMR in the uniform texture and in the d -soliton

To obtain frequency of the uniform NMR in the uniform texture we put $\alpha = 0$ in (39). Then the frequency is

$$\omega_u = \sqrt{\omega_L^2 + \Omega_P^2 \cos^2 \mu}. \quad (40)$$

This formula can be used to measure Ω_P .

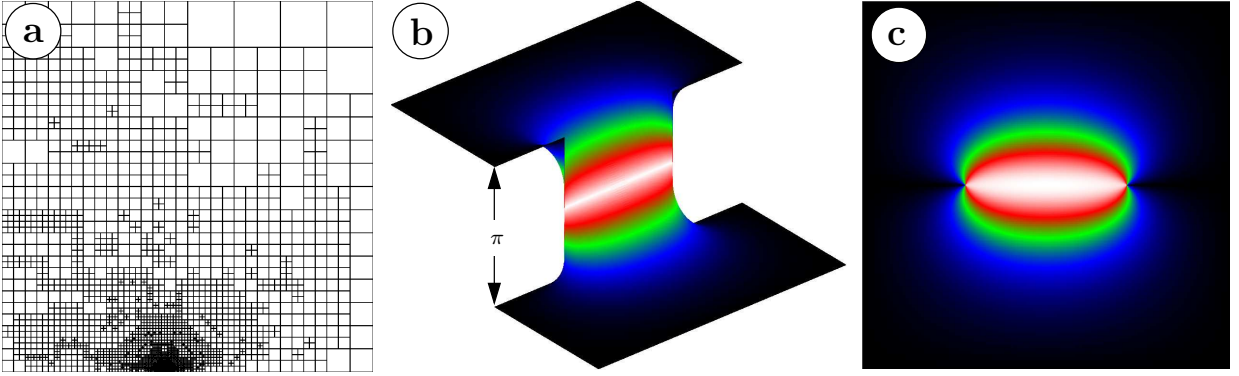


Fig. 4. An example of the calculated texture and the spin wave in the soliton between two half-quantum vortices. (a) The calculation grid made of 4696 cells covers one-fourth of the whole area $(8 \times 8)\bar{\xi}$ with two vortices separated by $D = 3.5\bar{\xi}$. Density of the grid is chosen according with gradients of the texture, it is higher near vortices. (b) Calculated value of α . One can see a smooth rotation by π in the soliton between vortices and π jump on the other side of vortices where phase also changes by π . (c) The calculated real-value wave \bar{s}_+ .

To find the spin wave, localized in the single d -soliton we use (39) and the soliton equation (22) for the distribution of α . This gives us

$$\bar{s}_+ = \cosh^{-1}(x/\bar{\xi}), \quad (41)$$

where as in (22) the value of $\bar{\xi}$ depends on the domain wall orientation. The frequency is

$$\omega_s = \sqrt{\omega_L^2 + \Omega_P^2 \cos 2\mu}. \quad (42)$$

On NMR experiments two peaks are observed, one from the uniform texture and another from waves localized in solitons. The difference between peak frequencies is

$$\delta\omega \approx \frac{\Omega_P^2}{2\omega} \sin^2 \mu \quad (43)$$

Intensity of the soliton peak (for a uniform rf-field) is proportional to the oscillator strength ([11]), the ratio

$$I^M = \frac{|\int_V s_+|^2}{\int_V |s_+|^2}. \quad (44)$$

This ratio also connects the total transverse magnetization, measured in NMR experiments $M_\perp = \gamma \int_V s_+$ and energy stored in the wave $E = \gamma^2/2\chi_\perp \int_V |s_+|^2$. Ratio I^M has a dimension of volume. For a localized wave it is approximately equal to the volume occupied by the wave. In one-dimensional case I^M has a dimension of length; for a single soliton (41) $I^M = 2\bar{\xi}$.

Numerical study of soliton structures

For understanding results of real NMR experiments it is important to study how various effects can change

the frequency of the wave localized in the soliton. We do it numerically in one and two-dimensional cases. Using coordinates in units of $\bar{\xi}^2$ one can write the equation (19) for the texture as

$$\nabla^2 \alpha = \frac{1}{2} \sin 2\alpha, \quad (45)$$

and equation (39) for the real-value waves as:

$$-\nabla^2 \bar{s}_+ + U(x) \bar{s}_+ = \lambda \bar{s}_+, \quad (46)$$

where potential $U(x) = -(\nabla\alpha)^2 - \sin^2 \alpha$ and

$$\lambda = \frac{\omega^2 - \omega_L^2 - \Omega_P^2 \cos^2 \mu}{\Omega_P^2 \sin^2 \mu} = -\frac{\omega^2 - \omega_u^2}{\omega_s^2 - \omega_u^2}. \quad (47)$$

In the case of a single soliton $\omega = \omega_s$ and $\lambda = -1$.

Using the equation (45) we can numerically calculate distribution of α . Then, using equation (46) we can calculate eigenvalues λ .

First consider a 1D periodic structure of parallel solitons, located at some distance D from each other. Solitons have an orientation (direction of $\nabla\alpha$), and two simplest structures which we study are sequences of solitons with same and alternating orientations.

The solution for this problem is shown on Fig. 3. Parameter λ for both periodic structures has the same value -1 as for the single soliton.

Let's also study an effect of a finite-length soliton. Consider a two-dimensional problem with two half-quantum vortices parallel to the l vector. Distance between vortices is D . The same equations (45) and (46) are solved numerically in 2D space using *deal.II* library [12]. The code is available in [13]. An example of the calculation is presented on Fig. 4.

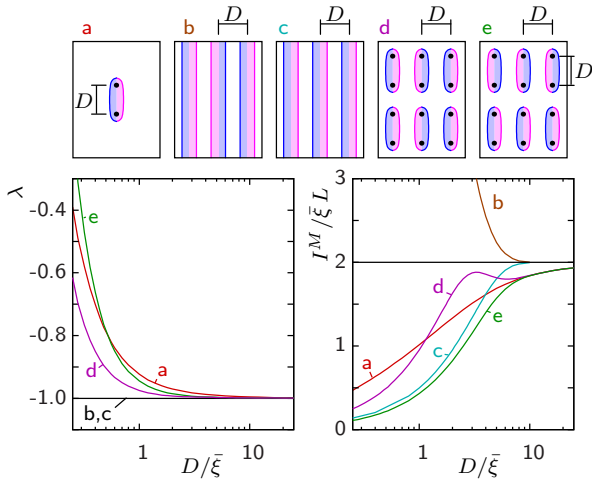


Fig. 5. Calculated values of λ and $I^M/\bar{\xi}L$ for various soliton structures. L is the total soliton length.

Near a half-quantum vortex, at a distance much smaller than $\bar{\xi}$, the textural angle $\alpha \approx \varphi/2 + \text{const.}$, where φ is the azimuthal coordinate. One can see that the potential in (46) is $U(x) \approx (\nabla\alpha)^2 \approx 1/4r^2$ (where r is distance from the vortex core). The real-value wave \bar{s}_+ can not fall into this hole because of Aharonov-Bohm effect: it should be zero along some radial direction to allow a smooth s_+ distribution. The symmetry reasons tell, that in the case of two vortices with a soliton the wave is zero on the line connecting vortices outside them. The corresponding solution of the wave equation is $\bar{s}_+ \approx \cos(\phi/2 + \text{const.})$, this kind of discontinuity is clearly seen on the calculated wave near vortices.

On Fig. 5 calculated values of λ and $I^M/\bar{\xi}L$ (L is the total soliton length) are plotted as a function of some structure dimension $D/\bar{\xi}$. There are five structures which are shown on the upper part of the figure: a single soliton with a finite length D ; A periodic structures of infinite solitons with the period D and same or alternating soliton orientations; the combination of both effects, periodic structures of finite solitons with equal length and period (this corresponds to a square lattice of vortices). For large D all curves come to the values for a single infinite soliton: $\lambda = -1$, $I^M = 2\bar{\xi}L$. A noticeable deviation of λ from the asymptotic value appears only at high vortex densities, when the inter-vortex distance D is comparable with $\bar{\xi}$.

Conclusion

Theoretical study of the texture and spin dynamics of the polar phase is done. We start with the polar

phase order parameter and the energy with magnetic, spin-orbit and gradient terms. The order parameter contains both orbital and spin anisotropy axes. The first one is fixed by the aerogel strands, and the second can move in the plane perpendicular to the applied magnetic field. Thus we have only one variable for the texture, an angle α . By minimizing the energy we get an equation for the equilibrium texture. It has a form of a static sine-Gordon equation for the angle α . We discuss possible topological defects in this texture: d -solitons, half- and one-quantum vortices. Characteristic length scale of the texture strongly depends on the angle μ between the magnetic field and aerogel strands. By rotating the magnetic field one can vary it from a $\xi_D \approx 20 \mu\text{m}$ to infinity.

Numerical simulations of various textures with half-quantum vortices are done. It is shown how interaction between vortices can change the NMR frequency.

Acknowledgements

I thank G.E. Volovik for useful discussions. This work has been supported in part by the Academy of Finland (project no. 284594).

1. K. Aoyama, R. Ikeda, *Phys. Rev. B*, **73**, 060504 (2006)
2. V.V. Dmitriev, A.A. Senin, A.A. Soldatov, A.N. Yudin, *Phys. Rev. Lett.*, **115**, 165304 (2015),
3. G. E. Volovik, V. P. Mineev, *JETP Lett.*, **24**, 561 (1976)
4. S. Autti, V.V. Dmitriev, V.B. Eltsov, J. Mäkinen, G.E. Volovik, A.N. Yudin, V.V. Zavjalov, *Phys. Rev. Lett.*, **117**, 255301 (2016),
5. V. P. Mineev, *J. Low Temp. Phys.*, **184**, 1007 (2016)
6. O. Hudak, *Phys. Lett.*, **89A**, 245 (1982).
7. A. Nakamura, *J. Phys. Soc. Jpn.*, **52**, 1918 (1983).
8. I.E. Dzyaloshinskii and G.E. Volovik, *Annals of Physics*, **125**, 67 (1980)
9. Y. Aharonov, D. Bohm, *Phys. Rev.*, **115** 485 (1959)
10. M. M. Salomaa and G. E. Volovik, *Rev. Mod. Phys.*, **59**, 533 (1987)
11. Chia-Ren Hu, Kazumi Maki, *Phys. Rev. B*, **36**, 6871 (1987)
12. <https://www.dealii.org>
https://github.com/slazav/dealii_progs